Evidence for, and an Understanding of, the Initial Nucleation of Carbon Nanotubes Produced by a Floating Catalyst Method

Wencai Ren, Feng Li, and Hui-Ming Cheng*

Shenyang National Laboratory for Materials Science, Institute of Metal Research, Chinese Academy of Sciences, 72 Wenhua Road, Shenyang 110016, China

Received: April 25, 2006; In Final Form: June 26, 2006

An understanding of the growth mechanism of carbon nanotubes (CNTs) is very important for the control of their structures, which in turn will be the basis for their further theoretical studies and applications. On the basis of high-resolution transmission electron microscopy observations of the initial nucleation of CNTs, the following deductions are made: (1) the nucleation of single-walled carbon nanotubes (SWNTs) and double-walled carbon nanotubes (DWNTs) starts at a low-temperature zone in front of the reaction zone; (2) the addition of sulfur results in localized liquid zones on the surface of big catalyst particles as the initial nucleation sites; (3) a temperature gradient is necessary to realize the role of sulfur in the structure of CNTs; and (4) the shell number of CNTs can be changed at the nucleation and growth stages. On the basis of the above, a growth model for the formation of SWNTs and DWNTs is proposed, which might open up the possibility of controlling the structure of CNTs.

1. Introduction

Some achievements have been obtained in the structural control of carbon nanotubes (CNTs), such as the diameter, shell number, organization, and orientation.[1−26] Single-walled carbon nanotubes (SWNTs),[1−4] double-walled carbon nanotubes (DWNTs),[5−8] multiwalled carbon nanotubes (MWNTs),[9−11] their aligned ropes[12−17] and arrays,[18−22] and individual SWNTs[23−26] can be selectively grown. These experimental advancements promote the further understanding of the mechanism of CNTs. Different growth models have been proposed to elucidate the growth of CNTs prepared by different methods, according to the experimental investigations and theoretical calculations. They follow either an opened-tip or closed-tip growth model depending on their tip structure,[27,28] or follow either a tip-growth or root-growth mechanism according to the position of catalysts,[29] or follow either a vapor−liquid−solid (VLS)[30] or solid−liquid−solid (SLS)[31] growth mechanism on the basis of the state of carbon source, during the growth process of CNTs.

The floating catalyst method is a very popular and effective approach for the controllable synthesis of CNTs in an expected large scale.[3,4,7,8,10−12,14,15,17,29,32,33] Further advancement of this approach to the controllable synthesis of CNTs requires a clear understanding of their growth mechanism. Generally, the formation of CNTs consists of three stages: nucleation, growth, and termination. Although the melting point of bulk catalyst metal is much higher than reaction temperatures, the nanoscale catalyst particles involved in the CNT synthesis are in a molten state even at a temperature far below their melting point, since the melting point of metallic particles can be reduced by (1) size effect[34] and (2) the solution of carbon.[31] Therefore, we consider that the VLS growth mechanism is responsible for the growth stage of CNTs for this method.[30] When the catalysts are entirely surrounded by graphitic layers, the growth of CNTs will terminate due to the disappearance of the activity sites of catalysts. In contrast to the latter two stages, the nucleation is the first step for their formation and crucial for CNT structural control. Moreover, it is much more complex.

In our previous paper, we systematically studied the effect of sulfur on the structures of CNTs and reported the growth of CNTs with controllable shell number and diameter distribution in one system.[32] Furthermore, based on the experimental parameter study results, high-resolution transmission electron microscopy (HRTEM) observations, and kinetic considerations, the role of sulfur in the growth of CNTs was discussed. Five main conclusions were drawn as follows:[32]

(1) The addition of sulfur is necessary to enhance the growth of SWNTs and DWNTs, independent of carbon source for our method, due to the formation of large catalysts for the growth of SWNTs and DWNTs.

(2) The growth of closed SWNTs starts from the formation of the cap-like structures.

(3) From the kinetic consideration, the nucleation and diameter of SWNTs and DWNTs with closed tips are considered to be changed by the addition of sulfur, through the resulting introduction of defects in the graphitic layer on the surface of catalysts and the alteration of surface energy of the sheet.

(4) The activity of catalysts was changed with the addition of sulfur due to the surface reconstruction of catalysts, which leads to the change of shell numbers of CNTs.

(5) The shell number of CNTs was related to carbon supply and diameters of CNTs.

It should be pointed out that the previous studies on the role of sulfur were mainly based on the kinetic considerations. Unfortunately, some basic information about the initial nucleation of CNT formation is still unclear, for example:

(1) When does the initial nucleation of SWNTs start?

(2) Which mechanism is responsible for the initial nucleation of SWNTs?

(3) Are the tips of SWNTs always closed at the initial nucleation stage?

* Address correspondence to this author. Fax: +86 24 23903126. E-mail: cheng@imr.ac.cn.

10.1021/jp062526x CCC: $33.50
Published on Web 08/10/2006

(4) What is the key factor for realizing the role of sulfur on the initial nucleation of SWNTs?

(5) Can the shell number be changed in the initial nucleation stage of CNTs?

In this paper, we will provide some evidence and get an insight into the initial nucleation of SWNTs and DWNTs, based on the experimental results and HRTEM observations.

2. Experimental Section

The floating catalyst method and the apparatus used were described in our previous work.[3] Here, methane or ethanol was used as the carbon source, ferrocene as the catalyst precursor, and thiophene as the growth promoter. In these experiments, the temperature of thiophene was maintained at 25 °C, and the typical reaction time was 5 min. The morphology and microstructure of the products were characterized by using HRTEM (JEOL 2010 200 kV) and Raman spectroscopy (Jobin Yvon LabRam HR800, excited by 632.8 nm laser).

3. Results and Discussion

3.1. When Does the Initial Nucleation of SWNTs Start? To determine the start of the initial nucleation of SWNTs, we studied the effect of temperature on their structures using methane as the carbon source and the results are presented as follows: no SWNTs were found at temperatures lower than 800 °C; a few SWNTs can be formed at the temperature of 900 °C; and the SWNT yield was increased with increasing the reaction temperature in the range of 900−1100 °C.

Therefore, we deduce that (1) the initial nucleation of SWNTs starts at a temperature lower than 900 °C, i.e., before the reaction zone, for methane as the carbon source, and (2) the high reaction temperature promotes the growth of SWNTs by enhancing the decomposition rate of methane and diffusion rate of carbon in the catalyst particles.

As we reported before,[32] sulfur is a crucial factor for the formation of SWNTs and DWNTs, since few of them can be formed without the addition of sulfur, and their diameters are closely dependent on the addition amount of sulfur. This leads us to propose a sulfur-assisted nucleation mechanism for the SWNTs and DWNTs prepared by our method. From these experimental facts, we infer that the decomposition temperature of thiophene is the possible temperature lower limit for starting the role of sulfur on the structure of CNTs. Therefore, the reaction sequence that happened in the reaction system should be analyzed to further verify the above deduction about the low-temperature nucleation. Here is some basic information about the three reactants used in our reaction system: The decomposition temperature of ferrocene is ∼470 °C.[35] The decomposition temperature of thiophene is not lower than 850 °C without the presence of catalyst.[36] However, the decomposition temperature may be greatly decreased in the presence of catalyst.[37−39] Methane is the most kinetically stable hydrocarbon at elevated temperature. No reports were found that methane can be catalytically decomposed to form SWNTs below 900 °C with iron as catalyst. Moreover, previous research indicated that its self-pyrolysis becomes stronger at ∼1000 °C only after a long reaction time.[23,40]

Therefore, we consider that the reactions that happened in the system follow a specific time sequence. First, ferrocene is decomposed at ∼470 °C to form small iron clusters or particles by collision in the floating gas. Second, thiophene is adsorbed and decomposed at some sites on the surface of iron particles at a temperature lower than 850 °C. Third, methane is catalytically decomposed on the surface of the catalysts to start the growth of CNTs. Apparently, the above analysis verifies that the proposed low-temperature nucleation is reasonable. It is worth noting that the nucleation mechanism for our method is quite different from that proposed for the arc-discharge method,[41−43] in which CNTs were considered to be formed due to the precipitation of carbon from the carbon-supersaturated catalysts when they were transferred from the high-temperature zone to the low-temperature zone.

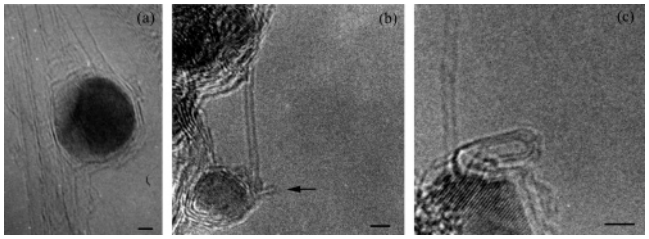

Figure 1. HRTEM images of individual SWNTs and the attached catalysts. The arrow in panel b denotes a very small SWNT with a diameter of ∼0.5 nm and closed tip. Scale bar: 2 nm.

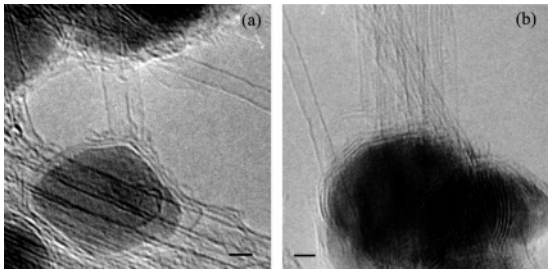

Figure 2. HRTEM images of SWNT bundles and the related catalysts. Scale bar: 2 nm.

3.2. Which Mechanism Is Responsible for the Initial Nucleation of CNTs? In this section, we will discuss how sulfur realizes its role in the initial nucleation of CNTs. Figure 1 shows several HRTEM images illustrating the correlations between catalysts and CNTs. It is worthy of note that the catalyst sizes are much larger than the diameters of the attached SWNTs. Similarly, SWNT bundles also grow from big catalysts (Figure 2), as reported for the SWNTs prepared by the arc discharge method.[42,43] Moreover, the catalysts with a diameter smaller than 2.0 nm (general diameters of as-prepared SWNTs and DWNTs) were rarely found during careful HRTEM observations. These results indicate a different nucleation mechanism from those of the HiPco[4,44] and CVD process,[45,46] in which the "Yarmulke" mechanism[45] was adopted based on the fact that the diameters of the SWNTs obtained are similar to the catalyst size. That is, SWNTs nucleate from these nanoscale particles by the initial formation of a small cap with a similar curvature. On the basis of the above correlation between the CNT diameters and the catalyst sizes, we propose that SWNTs or DWNTs nucleate from a localized zone of catalysts for our method. Therefore, the central problem of the initial nucleation is (1) how these localized zones are formed on a big catalyst and (2) how to nucleate SWNTs from the localized zones.

Previous studies indicate that thiophene usually preferentially adsorbs and dissociates at the defect sites on the surface of catalyst particles.[47] Moreover, it is well-known that sulfur can lead to the reconstruction of the surface of catalyst particles, consequently enhancing the catalytic activity.[48−50] Therefore, methane is preferentially decomposed at these sites due to the enhancement of their activity. Theoretical studies indicate that the structural symmetry of small size catalysts has a strong influence on their melting point.[51] The introduction of sulfur

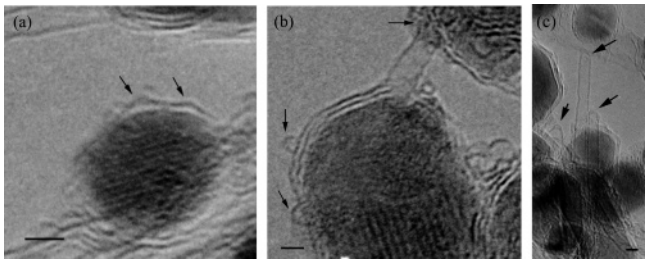

Figure 3. HRTEM images of the tip structure of closed SWNTs. The tips are denoted by an arrow. Scale bar: 2 nm.

and carbon atoms removes the symmetry of the corresponding zone, thereby reducing the melting point. Moreover, from the Fe−C−S phase diagram, the addition of sulfur can result in a reduction of the melting temperature of pure Fe and F−C alloy. Previous research indicated that the melting point of an $Fe_{500-m}C_m$ cluster decreases ∼150 °C compared to Fe_{500} as the carbon content in the cluster reaches 10−12%.[51] Therefore, localized liquid zones are expected to be formed on the surface of a big catalyst particle at low temperatures due to the introduction of sulfur and carbon. The rest region of the same catalyst remains solid due to a higher melting point for pure iron and few methane was decomposed at these areas due to low temperature and their low catalytic activity.

When the localized liquid zone is supersaturated in carbon due to high catalytic activity, some graphite islands can be preferentially precipitated at these areas as the initial nucleation sites for the growth of CNTs, via the VLS growth mechanism. Therefore, this localized zone is considered as the initial nucleation zone. Actually, this result is consistent with the low-temperature nucleation. That is, the nucleation can occur only at the localized zone instead of at the whole big catalyst particle at low carbon supply resulting from low temperature, due to the requirement of the precipitation of carbon, i.e., supersaturation of carbon in the particles. The high temperature enhances the decomposition of methane to produce more carbon supply and provides sufficiently high kinetic energy to overcome the attractive forces between the particle and graphite islands.[52] Therefore, the graphite islands will lift off the catalyst to form a cap-like structure (Figure 3) with the help of defects, as we elucidated previously,[32] when the catalysts are carried to the higher temperature zone by gas flow. It is worth noting that the time exhaust in an order of magnitude of nanoseconds is sufficient from the penetration of carbon into the iron particles with a diameter of 1 nm to the lift-off of the formed graphitic islands at 1000 K (727 °C), according to molecular dynamics (MD) simulation results.[53] This result further verifies that it is reasonable to form the cap-like structures before the catalysts are carried to the reaction zone.

According to the above nucleation mechanism, the area of the localized liquid zone is expected to be changed with different sulfur addition amounts, consequently changing the nucleation size, i.e., diameters of CNTs. It is interesting to note that the outer diameters of CNTs were increased with increasing the addition amount of sulfur, and approximately the area ratio (corresponding to the mean outer diameters, i.e., $S_{CNT} = \pi d_{outer}^2/4$) of SWNTs and DWNTs approaches that of the corresponding addition amount of sulfur.[32] This agreement strongly indicates that the *localized liquid zone nucleation mechanism* induced by sulfur is reasonable.

3.3. Are the Tips of CNTs Always Closed at the Initial Nucleation Stage? Figure 3a,b shows two HRTEM images at the initial nucleation stage of the formation of SWNTs, in which the bending of the graphite islands on the surface of the catalyst

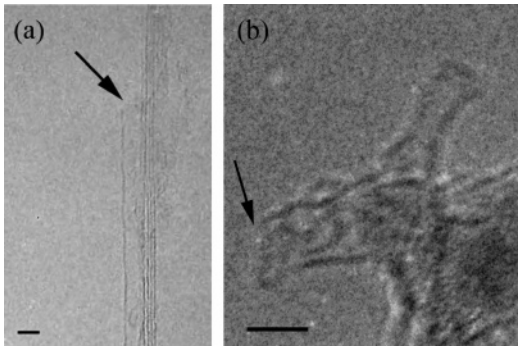

Figure 4. HRTEM images of opened SWNTs (denoted by arrows). Scale bar: 2 nm.

can be easily observed. Moreover, a small cap can be found at the opposite tip of each grown SWNTs to the catalyst (Figure 3c), even for the very small SWNT with a diameter of ∼0.5 nm, denoted by the arrow in Figure 1b. These observations further verify that (1) the closed SWNTs nucleate from the localized zone and (2) the growth of closed SWNTs starts from the formation of a cap-like structure from the bending of the graphite islands.[32]

However, several opened tips were also occasionally found, as shown in Figure 4. We believe that the difference of the tip structure can be attributed to the perturbation of the initial nucleation stage. Actually, it is possible to form opened CNTs since the interfaces between the solid and localized liquid zones are also the active sites for nucleation. Therefore, there should be a selection of carbon atom segregation between these sites and the surface of liquid zones depending on the carbon supply rate, the localized zone size, the temperature, etc., which determines the tip structure of the SWNTs and DWNTs synthesized by this method. Maruyama et al.[54,55] studied the initial nucleation of the SWNT by MD simulations and found that it is possible for an annular graphitic sheet to grow up from the circumferential edge of the metal−carbon cluster with an opened structure at the initial nucleation stage. This result provides theoretical support for our assumption. However, further investigations on the growth of CNTs are required to justify this deduction, especially through in situ TEM observations.

3.4. What Is the Key Factor for Realizing the Role of Sulfur on the Initial Nucleation of CNTs? According to our previous results, sulfur is very important for enhancing the growth of CNTs because of the larger size of catalysts than those of CNTs.[32] For realizing the role of sulfur, two other viewpoints we point out are (1) the delay of catalysts before the reaction zone makes it necessary to add sulfur to enhance the nucleation of SWNTs and DWNTs and (2) the temperature gradient is necessary to realize the role played by sulfur in our method. Without delay, the catalysts may remain at a suitable size for the growth of SWNTs and DWNTs, instead of further accumulation by collision. That is also the reason that a large amount of SWNTs with high purity can be obtained by using the closed-loop reactor in the HiPco method, since small catalysts with a suitable size for the growth of SWNTs can be stabilized without delay in the reactor for a long time, avoiding further accumulation of catalysts.[44] Therefore, it is not necessary to add sulfur to enhance the nucleation for SWNTs and DWNTs. However, without a water-cooler injector, only a few SWNTs and many MWNTs can be obtained because of the further growth of catalysts in the temperature gradient.[44] For the same reason, sulfur is also not necessary for the substrate CVD method, since the catalysts are small and have fixed sizes.[45,46]

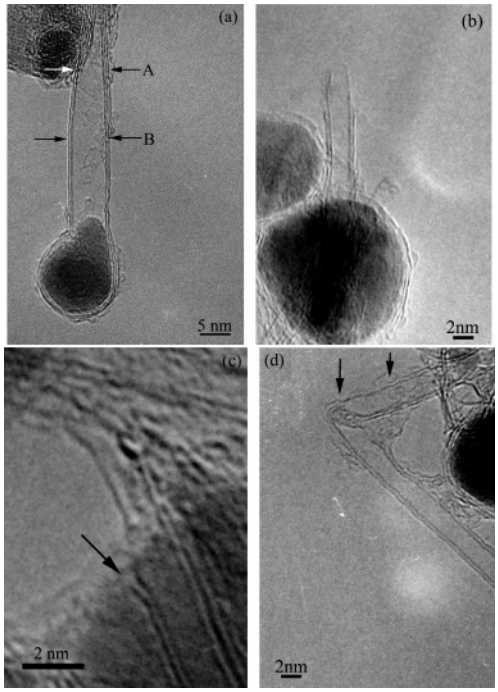

Figure 5. HRTEM images of DWNTs with a variation of shell number. The arrow in panels c and d denotes the variation position.

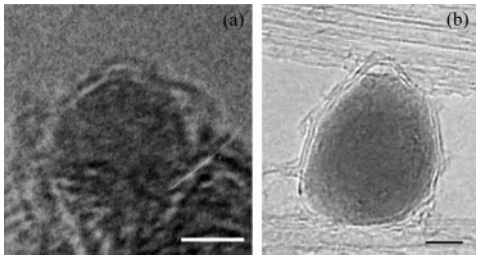

Figure 6. (a) The initial nucleation structure of closed DWNTs. (b) The tip structure of a closed DWNT. Scale bar: 2 nm.

Without the temperature gradient, the localized liquid nucleation zone for SWNT growth cannot be preferentially formed, since the whole catalyst becomes liquid almost simultaneously at reaction temperature. On the basis of the energy calculation of a large graphitic layer or graphite capsule entirely surrounding the catalyst relative to a SWNT,[56] these two structures were preferentially formed through a bulk diffusion of carbon instead of SWNTs, considering the catalyst size in our sample. Therefore, in this case, MWNTs or catalytic particles surrounded by graphitic layers were formed depending on the carbon supply rate. Therefore, we can conclude that the temperature gradient provides some time to stabilize the localized zone for the nucleation of SWNTs and for the graphite islands to lift off the catalyst avoiding their further outspread, so that it is crucial to realize the role of sulfur in the formation of SWNTs. Consequently, the growth of SWNTs is promoted by the addition of sulfur, due to the increase of nucleation sites suitable for the growth of SWNTs.

3.5. Can the Shell Number Change Occur in the Initial Nucleation Stage of CNTs? Here we will discuss the control of shell numbers of CNTs. Figures 5a,b and 6 show the correlation between DWNTs and the attached catalysts. It is apparent that the DWNTs follow the same *localized nucleation mechanism at low temperature* with SWNTs. Previous research indicates that MWNT growth is thought to be limited by the diffusion of carbon through catalyst particles,[57] and the growth of SWNTs and DWNTs is determined by a supply-limited reaction.[32,56] Therefore, the formation of DWNT is attributed to the change of carbon supply rate. Theoretically, the change of shell number can be predicted to occur either at the nucleation stage or at the growth stage of CNTs, attributed to the fact that the change of carbon supply can occur at the two stages.

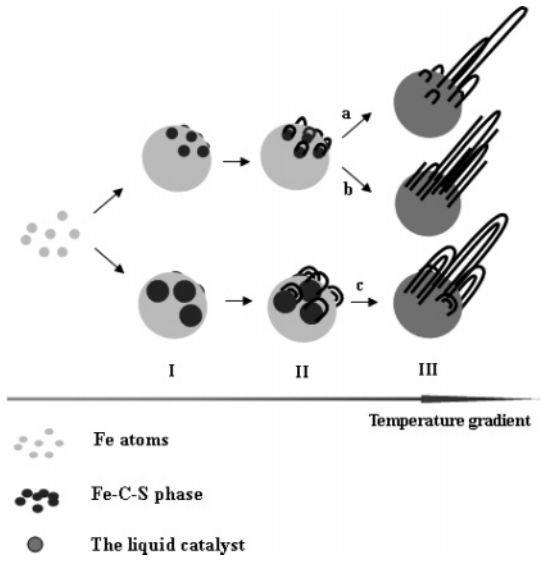

Figure 7. The diagram of the proposed growth model for SWNTs and DWNTs prepared by the sulfur-assisted floating catalyst method. I, II, and III represent the different temperature zone, respectively; a, b, and c represent the different formation routes for the CNTs with different structures, respectively.

Figure 5a shows a DWNT with a catalyst located at its tip. An obvious feature is that the shell number of this CNT varies accompanied by the change of diameter. Note that the shell number decreases as the diameter increases, and the carbon atoms of three walls at place A approximately approach to those of double walls at place B. These results provide evidence for a conclusion in our previous paper, that is, the shell number of CNTs is related to the carbon supply and the diameters of CNTs.[32] Moreover, two more pieces of experimental evidence for the shell number variation were found: (1) the inner tubes are longer than the outer ones for some DWNTs as shown in Figure 5b,c and (2) some DWNTs with a variation of shell number along the tube were also found in our experiment, denoted by an arrow in Figure 5d, and in general, only the outer layers are discontinuous. These three facts indicate that the shell number variation occurs during the growth stage.

Different from Figure 5, two caps can be formed with different curvatures at the initial nucleation stage for the closed DWNTs, as shown in Figure 6. We consider that this is attributed to the change of carbon supply at the initial nucleation stage of CNTs. Figure 6a shows the initial nucleation of closed DWNTs, in which the initial nuclei of the inner tube are still not lifted off the catalyst and are underneath the cap of the outer tube. Therefore, we deduce that the tip of the outer tube is bent with the help of the extrusion of the small graphitic layer below it in the case of high carbon supply, as stated for the formation of MWNTs in ref 41. All the above experimental results indicate that the shell number of CNTs can be changed at the nucleation and growth stages of CNTs.

3.6. The Growth Model for the SWNTs and DWNTs Prepared by the Sulfur-Assisted Floating Catalyst Method. Combining the above analysis, the nucleation and growth of SWNTs and DWNTs are schematically described in Figure 7. Here, we only present the formation of the closed SWNTs and DWNTs. In this figure, a, b, and c correspond to the formation

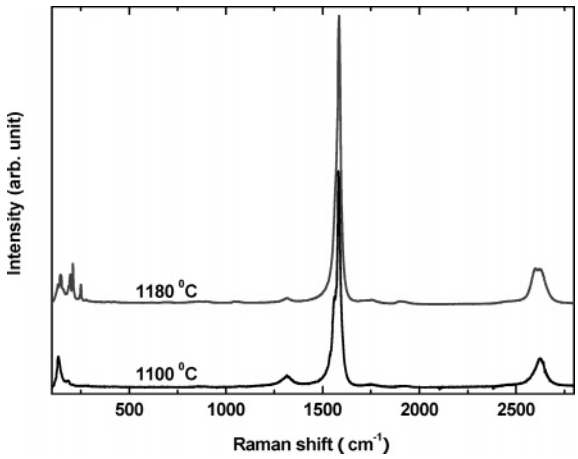

Figure 8. Resonant Raman spectra of CNTs prepared with a reaction temperature of 1100 and 1180 °C, respectively. Excitation laser energy: 1.96 eV.

of CNTs with a structure like Figure 3, Figure 5c, and Figure 6, respectively. It can be predicted from this growth model that the tip structure is determined in stage II for the SWNTs; the diameter is determined in stages I and III; and the shell number is determined in stages II and III. Therefore, we can purposively control the structure of CNTs, according to the function stage of different experimental parameters, such as the addition of sulfur, temperature gradient in the furnace, reaction temperature, carbon source content, and reaction gas composition. Here we give only one example, i.e., the effect of reaction temperature on the structure of CNTs, to demonstrate the utilization of this growth model.

Note that the change of reaction temperature mainly plays a role in stage III and can lead to a change of carbon supply to the surface of catalysts and carbon diffusion ability through catalysts. We believe that the diffusion ability is high enough in the present experimental conditions, based on the fact that MWNTs were formed instead of SWNTs and DWNTs with the addition of carbon source. Therefore, an alteration of shell number is expected to occur with a change in the reaction temperature. Figure 8 shows the resonant Raman spectra of the products synthesized at different reaction temperatures. In these comparative experiments, the flow rates of methane and hydrogen were kept at 250 and 1800 sccm, respectively. The sulfur addition amount was $\sim 1.00 \times 10^{-4}$ mol/min. It is apparent that some high-frequency radial breathing mode (RBM) peaks appear with the temperature increasing from 1100 to 1180 °C, indicating that some DWNTs were formed in the product.[5,7,17,32,58−61] Moreover, in this case, no substantial diameter change was found. These results can also be verified by the change of the line shapes and frequencies of the *G*-band and *G′*-band profiles.[60,61] These results are consistent with the above predictions based on the proposed growth model, indicating the reasonableness of this growth model. Of course, the shell number of CNTs can also be altered by changing the flow rate of the carbon source and the addition amount of sulfur, as reported in ref 32.

4. Conclusions

This paper presents some evidence for the initial nucleation stage of SWNTs and DWNTs produced by a floating catalyst method. On the basis of the experimental results and HRTEM observations, a *localized liquid zone nucleation mechanism at low temperature* was proposed and several viewpoints were addressed as follows: (1) the nucleation of SWNTs and DWNTs starts at a low-temperature zone before the reaction zone; (2) the addition of sulfur results in a localized liquid zone on the surface of big catalysts as initial nucleation sites, therefore the diameters of SWNTs and DWNTs are changed with the change of sulfur addition amount; (3) the temperature gradient plays a very important role in the effect of sulfur on the structure of CNTs; and (4) the shell number change of CNTs can be realized in the nucleation and growth stages. The results indicate that it is possible to realize the control of the structure of CNTs, such as the diameter and shell number, by changing the temperature gradient in the furnace, sulfur addition, reaction temperature, carbon source content, and reaction gas composition, based on the proposed growth model. These results open up a possibility for guiding the structure-controlled growth of CNTs.

Acknowledgment. The authors acknowledge Prof. M. Z. Wang and Dr. F. Ding for constructive advice and fruitful comments. This work is supported by NSFC grants (No. 90206018 and No. 50328204).

References and Notes

(1) Bethune, D. S.; Kiang, C. H.; Devries, M. S.; Gorman, G.; Savoy, R.; Vazquez, J.; Beyers, R. *Nature* **1993**, *363*, 605.
(2) Thess, A.; Lee, R.; Nikolaev, P.; Dai, H. J.; Petit, P.; Robert, J.; Xu, C. H.; Lee, Y. H.; Kim, S. G.; Rinzler, A. G.; Colbert, D. T.; Scuseria, G. E.; Tomanek, D.; Fischer, J. E.; Smalley, R. E. *Science* **1996**, *273*, 483.
(3) Cheng, H. M.; Li, F.; Su, G.; Pan, H. Y.; He, L. L.; Sun, X.; Dresselhaus, M. S. *Appl. Phys. Lett.* **1998**, *72*, 3282.
(4) Nikolaev, P.; Bronikowski, M. J.; Bradley, R. K.; Rohmund, F.; Colbert, D. T.; Smith, K. A.; Smalley, R. E. *Chem. Phys. Lett.* **1999**, *313*, 91.
(5) Bandow, S.; Takizawa, M.; Hirahara, K.; Yudasaka, M.; Iijima, S. *Chem. Phys. Lett.* **2001**, *337*, 48.
(6) Hutchison, J. L.; Kiselev, N. A.; Krinichnaya, E. P.; Krestinin, A. V.; Loutfy, R. O.; Morawsky, A. P.; Muradyan, V. E.; Obraztsova, E. D.; Sloan, J.; Terekhov, S. V.; Zakharov, D. N. *Carbon* **2001**, *39*, 761.
(7) Ren, W. C.; Li, F.; Chen, J.; Bai, S.; Cheng, H. M. *Chem. Phys. Lett.* **2002**, *359*, 196.
(8) Ci, L. J.; Rao, Z. L.; Zhou, Z. P.; Tang, D. S.; Yan, Y. Q.; Liang, Y. X.; Liu, D. F.; Yuan, H. J.; Zhou, W. Y.; Wang, G.; Liu, W.; Xie, S. S. *Chem. Phys. Lett.* **2002**, *359*, 63.
(9) Ebbesen, T. W.; Ajayan, P. M. *Nature* **1992**, *358*, 220.
(10) Sen, R.; Govindaraj, A.; Rao, C. N. R. *Chem. Mater.* **1997**, *9*, 2078.
(11) Fan, Y. Y.; Li, F.; Cheng, H. M.; Su, G.; Yu, Y. D.; Shen, Z. H. *J. Mater. Res.* **1998**, *13*, 2342.
(12) Cheng, H. M.; Li, F.; Sun, X.; Brown, S. D. M.; Pimenta, M. A.; Marucci, A.; Dresselhaus, G.; Dresselhaus, M. S. *Chem. Phys. Lett.* **1998**, *289*, 602.
(13) Liu, C.; Cheng, H. M.; Cong, H. T.; Li, F.; Su, G.; Zhou, B. L.; Dresselhaus, M. S. *Adv. Mater.* **2000**, *12*, 1190.
(14) Zhu, H. W.; Xu, C. L.; Wu, D. H.; Wei, B. Q.; Vajtai, R.; Ajayan, P. M. *Science* **2002**, *296*, 884.
(15) Li, Y. L.; Kinloch, I. A.; Windle, A. H. *Science* **2004**, *304*, 276.
(16) Zhang, M.; Atkinson, K. R.; Baughman, R. H. *Science* **2004**, *306*, 1358.
(17) Ren, W. C.; Cheng, H. M. *J. Phys. Chem. B* **2005**, *109*, 7169.
(18) Li, W. Z.; Xie, S. S.; Qian, L. X.; Chang, B. H.; Zou, B. S.; Zhou, W. Y.; Zhao, R. A.; Wang, G. *Science* **1996**, *274*, 1701.
(19) Ren, Z. F.; Huang, Z. P.; Xu, J. W.; Wang, J. H.; Bush, P.; Siegal, M. P.; Provencio, P. N. *Science* **1998**, *282*, 1105.
(20) Fan, S. S.; Chapline, M. G.; Franklin, N. R.; Tombler, T. W.; Cassell, A. M.; Dai, H. J. *Science* **1999**, *283*, 512.
(21) Murakami, Y.; Chiashi, S.; Miyauchi, Y.; Hu, M. H.; Ogura, M.; Okubo, T.; Maruyama, S. *Chem. Phys. Lett.* **2004**, *385*, 298.
(22) Hata, K.; Futaba, D. N.; Mizuno, K.; Namai, T.; Yumura, M.; Iijima, S. *Science* **2004**, *306*, 1362.
(23) Kong, J.; Soh, H. T.; Cassell, A. M.; Quate, C. F.; Dai, H. J. *Nature* **1998**, *395*, 878.
(24) Dai, H. J. *Acc. Chem. Res.* **2002**, *35*, 1035.
(25) Huang, S. M.; Cai, X. Y.; Liu, J. *J. Am. Chem. Soc.* **2003**, *125*, 5636.
(26) Zheng, L. X.; O'Connell, M. J.; Doorn, S. K.; Liao, X. Z.; Zhao, Y. H.; Akhadov, E. A.; Hoffbauer, M. A.; Roop, B. J.; Jia, Q. X.; Dye, R. C.; Peterson, D. E.; Huang, S. M.; Liu, J.; Zhu. Y. T. *Nat. Mater.* **2004**, *3*, 673.
(27) Saito, R.; Fujita, M.; Dresselhaus, G.; Dresselhaus, M. S. *Mater. Sci. Eng. B* **1993**, *19*, 185.

(28) Endo, M.; Kroto, H. W. *J. Phys. Chem.* **1992**, *96*, 6941.
(29) Hayashi, T.; Kim, Y. A.; Matoba, T.; Esaka, M.; Nishimura, K.; Tsukada, T.; Endo, M.; Dresselhaus, M. S. *Nano Lett.* **2003**, *3*, 887.
(30) Wagner, R. S.; Ellis, W. C. *Appl. Phys. Lett.* **1964**, *4*, 89.
(31) Gorbunov, A.; Jost, O.; Pompe, W.; Graff, A. *Carbon* **2002**, *40*, 113.
(32) Ren, W. C.; Li, F.; Bai, S.; Cheng, H. M. *J. Nanosci. Nanotechnol.* **2006**, *6*, 1339.
(33) Cao, A. Y.; Zhang, X. F.; Xu, C. L.; Liang, J.; Wu, D. H.; Chen, X. H.; Wei, B. Q.; Ajayan, P. M. *Appl. Phys. Lett.* **2001**, *79*, 1252.
(34) Buffat, P. A.; Borel, J.-P. *Phys. Rev. A* **1976**, *13*, 2287.
(35) Chem./Phy. Info, Merck KGaA, 803978, Ferrocene for synthesis.
(36) Material Safety Data Sheet, Thiophene, 99+%, ACC no. 91077.
(37) Stöhr, J.; Kollin, E. B.; Fischer, D. A.; Hastings, J. B.; Zaera, F.; Sette, F. *Phys. Rev. Lett.* **1985**, *55*, 1468.
(38) Morin, C.; Eichler, A.; Hirschl, R.; Sautet, P.; Hafner, J. *Surf. Sci.* **2003**, *540*, 474.
(39) Cheng, L. C.; Bocarsly, A. B.; Bernasek, S. L.; Ramanarayanan, T. A. *Surf. Sci.* **1997**, *374*, 357.
(40) Tibbetts, G. G. *Appl. Phys. Lett.* **1983**, *42*, 666.
(41) Kanzow, H.; Ding, A. *Phys. Rev. B* **1999**, *60*, 11180.
(42) Gavillet, J.; Loiseau, A.; Journet, C.; Willaime, F.; Ducastelle, F.; Charlier, J. C. *Phys. Rev. Lett.* **2001**, *87*, 275504.
(43) Gavillet, J.; Loiseau, A.; Ducastelle, F.; Thair, S.; Bernier, P.; Stephan, O.; Thibault, J.; Charlie, J. C. *Carbon* **2002**, *40*, 1649.
(44) NiKolaev, P. *J. Nanosci. Nanotechnol.* **2004**, *4*, 307.
(45) Dai, H. J.; Rinzler, A. G.; Nilolaev, P.; Thess, A.; Colbert, D. T.; Smalley, R. E. *Chem. Phys. Lett.* **1996**, *260*, 471.
(46) Li, Y. M.; Kim, W.; Zhang, Y. G.; Rolandi, M.; Wang, D. W.; Dai, H. J. *J. Phys. Chem. B* **2001**, *105*, 11424.
(47) Liu, G.; Rodriguez, J. A.; Dvorak, J.; Hrbek, J.; Jirsak, T. *Surf. Sci.* **2002**, *505*, 295.
(48) Rodriguez, N. M. *J. Mater. Res.* **1993**, *8*, 3233.
(49) Kim, M. S.; Rodriguez, N. M.; Baker, R. T. K. *J. Catal.* **1993**, *143*, 449.
(50) Owens, W. T.; Rodriguez, N. M.; Baker, R. T. K. *Catal. Today* **1994**, *21*, 3.
(51) Ding, F.; Bolton, K.; Rosén, A. *J. Vac. Sci. Technol. A* **2004**, *22*, 1471.
(52) Ding, F.; Bolton, K.; Rosén, A. *J. Phys. Chem. B* **2004**, *108*, 17369.
(53) Ding, F.; Bolton, K. *Nanotechnology* **2006**, *17*, 543.
(54) Shibuta, Y.; Maruyama, S. *Chem. Phys. Lett.* **2003**, *382*, 381.
(55) Maruyama, S.; Murakami, Y.; Shibuta, Y.; Miyauchi, Y.; Chiashi, S. *J. Nanosci. Nanotechnol.* **2004**, *4*, 360.
(56) Hafner, J. H.; Bronikowski, M. J.; Azamian, B. R.; Nikolaev, P.; Rinzler, A. G.; Colbert, D. T.; Smith, K. A.; Smalley, R. E. *Chem. Phys. Lett.* **1998**, *296*, 195.
(57) Baker, R. T. K.; Harris, P. S.; Thomas, R. B.; Waite, R. J. *J. Catal.* **1973**, *30*, 86.
(58) Li, F.; Chou, S. G.; Ren, W. C.; Gardecki, J. A.; Swan, A. K.; Unlu, M. S.; Goldberg, B. B.; Cheng, H. M.; Dresselhaus, M. S. *J. Mater. Res.* **2003**, *18*, 1251.
(59) Ren, W. C.; Li, F.; Cheng, H. M. *AIP Conf. Proc.* **2003**, *685*, 328.
(60) Ren, W. C.; Li, F.; Cheng, H. M. *Phys. Rev. B* **2005**, *71*, 115428.
(61) Ren, W. C.; Li, F.; Tan, P. H.; Cheng, H. M. *Phys. Rev. B* **2006**, *73*, 115430.